Supplementary methods, data, and figures

Macrophage-derived netrin-1 drives adrenergic nerve associated lung fibrosis

Authors: Ruijuan Gao,[1,2] Xueyan Peng,[1] Carrighan D. Perry,[1] Huanxing Sun,[1] Aglaia Ntokou,[3] Changwan Ryu,[1] Jose L. Gomez,[1] Benjamin C. Reeves,[1] Anjali Walia,[1] Naftali Kaminski,[1] Nir Neumark,[1] Genta Ishikawa,[1] Katharine E. Black,[4] Lida P. Hariri,[4,5] Meagan W. Moore,[1] Mridu Gulati,[1] Robert J. Homer,[1,6] Daniel M. Greif,[3,7] Holger K. Eltzschig,[8] and Erica L. Herzog [1,6*]

Affiliations:

[1]Section of Pulmonary, Critical Care, and Sleep Medicine, Department of Internal Medicine, Yale School of Medicine, New Haven, Connecticut, USA.

[2]Department of Oncology, Institute of Medicinal Biotechnology, Chinese Academy of Medical Sciences & Peking Union Medical College, No.1 Tiantan Xili, Beijing, China

[3]Section of Cardiology, Department of Internal Medicine, Yale School of Medicine, New Haven, Connecticut, USA.

[4]Division of Pulmonary and Critical Care Medicine, Massachusetts General Hospital, Harvard Medical School, Boston, Massachusetts, USA.

[5]Department of Pathology, Massachusetts General Hospital, Harvard Medical School, Boston, Massachusetts, USA.

[6]Department of Pathology, Yale School of Medicine, New Haven, Connecticut, USA.

[7]Department of Genetics, Yale School of Medicine, New Haven, Connecticut, USA.

[8]Department of Anesthesiology, University of Texas at Houston Medical School, Houston, Texas, USA.

Keywords: Pulmonary Fibrosis, Macrophage, Netrin-1, Adrenergic Nerve remodeling

This PDF file includes:

Materials and Methods

Animals. All experiments involving vertebrate animals were performed according to the principles approved by the Yale University Institutional Animal Care and Use Committee and were handled adhering to the Guide for the Care and Use of Laboratory Animals. C57BL/6J wild-type (WT), *Colα2-CreER* (Stock No. 029235), *LysMCre* (Stock No.: 004781), and $Dcc^{kanga/+}$(Stock No.: 029220) were purchased from Jackson Laboratory. $Ntn1^{fl/fl}$ (1) and $Ntn^{+/-}$ (2) mice were described previously. *Col1α2-CreER* mice express a tamoxifen (TAM)-inducible Cre recombinase driven by the mouse *Col1α2* collagen promoter and have been widely used for studies of fibrosis (3). TAM administration in double mutant mice induces Cre recombination in fibroblasts of numerous organs. *LysMCre* mice allow for Cre-mediated deletion of LoxP-flanked target genes in myeloid cells such as macrophages (4). $Dcc^{kanga/+}$ mice contain reduced *Dcc* but have no obvious phenotype. *LysMCre,* $Ntn1^{fl/fl}$ and *Col1α2-CreER,* $Ntn1^{fl/fl}$ mice were generated by crossing $Ntn1^{fl/fl}$ animals with the aforementioned corresponding Cre lines. After genotyping via polymerase chain reaction (PCR), the mice were separated and reserved in cages until the time of experimentation. All mice were maintained and bred in the AAALAC-accredited center at Yale University in New Haven, Connecticut.

Human studies. All human studies were performed with approval from institutional Human Investigation Committees at Yale University or Massachusetts General Hospital. Measurements of noradrenaline (NA) and adrenaline (A) occurred on explanted control or idiopathic pulmonary fibrosis (IPF) lung tissues obtained from The Yale Lung Repository (TYLR) and Massachusetts General Hospital. Netrin-1 (NTN1) and Mac1 immunohistochemistry on human lung tissue was performed on FFPE samples obtained from TYLR.

Drugs. Pharmacologic grade bleomycin was obtained from McKesson Medical Surgical, Inc (Wallingford, CT). 6-hydroxydopamine hydrochloride (6-OHDA, H4381), Terazosin hydrochloride (T4680), tamoxifen (TAM, T5648) and urethane (U2500) were purchased from Sigma-Aldrich (St. Louis, MO, USA). Isoflurane (50019100) was ordered from Zoetis Inc. (Kalamazoo, MI, USA). 1,2-propanediol (30948) was purchased from Alfa Aesar (Tewksbury, MA, USA).

Bleomycin model. For WT, *Ntn1*$^{fl/fl}$, *LysMCre, Ntn1*$^{fl/fl}$, *Col1α2-CreER, LysMCre, and Dcc*$^{kanga/+}$ mice, the bleomycin models were performed according to our previous description (5). Each mouse was anesthetized with 40% isoflurane and 60% 1,2-propanediol, exposed to a single dose of bleomycin (1.25 U/kg) via oropharyngeal aspiration and followed for 14 or 21 days. Sex-matched, saline challenged mice served as controls. Groups were evenly divided between males and females. To establish the bleomycin model using *Col1α2-CreER, Ntn1*$^{fl/fl}$ mice, mice were manually randomized to receive TAM or corn oil (Cat. No.: C8267, Sigma) for 7 days, allowed to rest for 7 days and treated with bleomycin as above. In all experiments, at the indicated timepoint, mice were terminally anesthetized with 18% urethane, and then bronchoalveolar lavage (BAL) was collected by delivering 0.8 ml cold PBS into the airway through a tracheal cannula and gently aspirating the fluid. The lavage was performed twice. BAL cells were centrifuged and resuspended in 100 μl of 1×PBS followed by cell counting. Subsequently, mouse lung tissues were lavaged with 1×PBS. Lungs were then processed for their respective endpoints.

Collagen quantification. Lung tissue was harvested for the determination of collagen content by Sircol™ Soluble Collagen Assay (S1000, Biocolor Ltd. NI, U.K.) according to our previous methods (6).

Vibratome sectioning and staining. Protocols are fully described in main text.

Determination of noradrenaline and adrenaline concentrations in BAL and lung tissues. Concentrations of noradrenaline (NA) and adrenaline (A) were determined in BAL and lung tissues using the commercialized noradrenaline and adrenaline high sensitivity ELISA kits (NOU39-K01 and ADU39-K01, DLD Diagnostika, GMBH, Hamburg, Germany) that have been used for this application in other publications (7). To improve the stability of NA and A, BAL samples were enriched with 1×PBS containing 10% Sample Stabilizer included in the kit before freezing at -80°C. Lung tissues were snap frozen and put into liquid nitrogen for temporary storage. After weighing, lung tissues were homogenized in 0.01 N HCl in the presence of 0.15 mM EDTA (AB00502, American Bioananlytical) and 4 mM sodium metabisulfite (13459, Sigma). After centrifuging for 10 minutes, the supernatants were collected for use. According to the instructions of the kits, NA and A in BAL and lung tissues were extracted using a cis-diol-specific affinity gel followed by acylation and enzymatic conversion. Competitive ELISA was performed, and the concentrations of NA and A were calculated using the curve of NA and A standards. Data from lung tissues were normalized to the wet weight of lung for each sample. The ratio of NA to A (NA/A) was then determined to adjust for the presence of adrenally derived NA.

Imaging mass cytometry

Prior to de-waxing, slides were air dried for at least 1 day at room temperature in a slide dryer. Slides were then de-waxed in fresh xylene for 7 minutes twice and subsequently hydrated in descending grades of ethanol (100% [twice], 95%, 80%, 70% and 50%) for 7 minutes each. Next, slides were washed in Milli-Q Water for 5 minutes twice in a Coplin jar and then incubated with preheated antigen retrieval solution (96 °C) for 30 minutes. Slides were then cooled to 70° C for 10 minutes and quickly washed with Milli-Q Water (twice) in a Coplin jar and DPBS for 5 minutes with gentle agitation. Tissue sections were blocked with 0.3% BSA in DPBS for 30 minutes at RT in a hydration chamber and then incubated overnight with the prepared antibody cocktail (Netrin-1-152Sm, CD11b-149Sm, F/480-159Tb, and HistoneH3-176Yb [to identify nuclei]) in 100ul DPBS at 4 °C in a hydration chamber. The next day, slides were washed in TBS-T (Tween-20, 0.05%) for 5 minutes (twice) with slow agitation in Coplin jars. Sections were stained with Ir-Intercalator in DPBS for 60 minutes at room temperature in a hydration chamber, then washed with TBS-T for 5 minutes (twice), then washed with Milli-Q water for 5 minutes (twice), and then allowed to air-dry for more than 30 minutes at room temperature. Slides were imaged with the Hyperion Imaging Mass Cytometer (8). Data were analyzed using open source HistoCAT software (9).

In vitro macrophage stimulation. Peritoneal macrophages were stimulated with 1 μg/ml LPS (Sigma, L2630) or 20 ng/ml recombinant mouse IL-13 **(**R&D Systems, 413-ML-005**).**

Enzyme linked immunosorbent assay (ELISA). Supernatants from LPS or IL-13 stimulated peritoneal macrophages underwent measurement of Chi3L1 (R&D Systems, MC3L10) or IL-13

(R&D Systems, M1300B) using well validated commercial assays as previously reported by our group (6).

Chemical sympathectomy. In order to determine whether the increase in NA was nerve-derived in bleomycin-challenged WT mice, chemical sympathectomy was performed to block the presynaptic release of NA according to the previous description of 6-OHDA as a specific sympathetic neurotoxin (10). Briefly, WT mice were randomly divided into two groups: one group was intraperitoneally treated with 100 mg/kg 6-OHDA dissolved in 0.9% NaCl containing 10^{-7} M L-ascorbic acid (A7506, Sigma) on day -7 and 50 mg/kg 6-OHDA on day -5, day -3, day 3, day 8 and day 11; another group served as vehicle mice which received only 0.9% NaCl containing 10^{-7} M L-ascorbic acid (A7506, Sigma) at the indicated timepoints. A single dose of bleomycin (1.25 U/kg) was orotracheally administered to each mouse at day 0. All mice were humanely sacrificed at day 14. BAL and lung tissues were collected for the determination of NA/A, TH+ nerve content, and soluble collagen using aforementioned methods.

Fluorescence activated cell sorting (FACS). Protocols are fully outlined in main text.

Terazosin treatment. Terazosin was used to block α1 adrenoreceptors at the postsynaptic level. Terazosin is a high affinity ADRA1 receptor antagonist used to treat hypertension and prostate disorders (11). Briefly, WT mice (7-9 weeks old) received a single dose of bleomycin (1.25 U/kg) or saline at day 0. Five days later, these mice were manually randomized into 2 groups. One group was intraperitoneally injected with 1 mg/kg Terazosin from day 5 to day 13; another group were synchronously treated with saline and served as vehicle controls. Mice were sacrificed at day 14.

In a separate set of studies, bleomycin exposed mice received Terazosin or vehicle starting at day 10 and continuing until day 21.

Histologic analysis, immunohistochemistry, and immunocytochemistry. Protocols are fully outlined in main text.

RNA extraction, cDNA synthesis and quantitative real-time PCR. Total RNA was isolated from mouse or human lung tissues using Direct-zol™ RNA MiniPrep Kit as described on the protocol (R2053, Zymo Research). RNA concentration was determined at 260 nm by NanoDrop 2000 and then reversely transcribed to generate cDNA using SuperScript®VILO™ cDNA Synthesis Kit (11754-050, Invitrogen). Quantitative real-time (qRT)-PCR was performed using the cDNA as the templates with the ABI real-time 7500 PCR system. The β-actin gene was used as an internal standard control. Relative quantification was then calculated using the $2^{-\Delta CT}$ method as previously reported by our lab (6).

The primers for mouse samples were:

Actb-F: 5′-ACCCTAAGGCCAACCGTGA-3′;

Actb-R: 5′-TGGCGTGAGGGAGAGCATAG-3′;

Dcc-F: 5′-GGATACCCGCATCCACAGTT-3′;

Dcc-R: 5′-GGCTGTGGGGATGGTTCTA-3′.

Human primers were as follows:

ACTB-F: 5′- GTGGGCCGCTCTAGGCACCA -3′;

ACTB-R: 5′-CGGTTGGCCTTAGGGTTCAGG-3′;

NTN1-F: 5′- CGCTGTGAAAAAGCCTGCAA-3′;

NTN1-R: 5′-GTACAGTTCGGTAGCATTCTGAC-3′

Western Blotting. To obtain lung tissue protein, lavaged lungs were directly homogenized and lysed in Pierce® RIPA buffer (89901, Thermo Scientific) containing 1×Phosphatase inhibitor cocktail (04906837001, Roche Diagnostics) on the ice for 30 minutes. In order to obtain lung macrophage protein, the whole lungs were enzyme-digested as above, and resulting cells suspended in 1×DPBS containing 0.5% BSA and 2 mM EDTA. Cells were then magnetically labeled with mouse anti-F4/80 microbeads (130-110-443, Miltenyi Biotec Inc.) and then subject to macrophage isolation through MS columns (130-042-201, Miltenyi Biotec Inc.) on an OctoMACS™ Separator (130-042-109, Miltenyi Biotec Inc.) attached to the MultiStand (130-042-303, Miltenyi Biotec Inc.) according to the company's protocol. The positively selected lung macrophages expressing mouse F4/80 antigen were further sonicated and lysed as aforementioned. The total protein were obtained in the form of the supernatant via centrifuging at 14,000 rpm for 30 minutes. The total protein concentration was determined with the Pierce™ BCA Protein Assay Kit (23225, Thermo Scientific). 10 μg of total proteins were resolved by SDS-PAGE in a 4-15% precast gel (4568084, Bio-Rad Laboratories) and then transferred onto a methanol-activated PVDF membrane using the Trans-Blot® Turbo™ RTA Transfer Kit (170-4273, Bio-Rad Laboratories). The membranes carrying the total proteins were blocked for at least 1 h at room temperature with 5% non-fat dry milk (AB10109-00100, americanBIO) /1×TBST Buffer (AB14330-01000, americanBIO) and then incubated overnight with the rabbit primary antibody directed against

NTN1 (ab126729, Abcam) at 4℃. Next day, the membranes were washed thrice with 1×TBST and then continuously incubated with HRP-labeled goat anti-rabbit IgG (G21234, Invitrogen) for 2 hours with a dilution of 1: 2000. The β-actin serving as a sample loading control was immunoblotted using the HRP-labeled Direct-Blot™ anti-β-actin (664804, Biolegend) with 1:10 000 dilutions at room temperature. The blots were developed using SuperSignal® West Femto Maximum Sensitivity Substrate (34096, Thermo Scientific), and the images were captured using ChemiDoc™ MP Imaging System with the Image Lab™ software version 5 (Bio-Rad Laboratories, Inc., Portland, ME, USA). The densitometric analyses were performed using the same Image Lab™ software based on the captured images.

TUNEL staining. Paraffin-embedded 5 μm sections from formalin fixed, paraffin embedded lung tissues were assessed using the TUNEL assay using the ApopTag® Peroxidase in Situ Apoptosis Detection Kit (S7100, EMD Millipore Corp) according to the manufacturer′s protocol. Briefly, the formalin-fixed, paraffin-embedded lung sections were deparaffinized in 100% xylene (8668, Avantor Performance Materials) and then rehydrated and treated with 20 μg/ml IHC Select® Proteinase K (21627, MilliporeSigma) for 15 minutes at room temperature. After quenching the endogenous peroxidase with 3% hydrogen peroxide (2186, Avantor Performance Materials), lung sections were equilibrated and then incubated with the reaction buffer containing terminal deoxynucleotidyltransferase in a humidified chamber at 37℃ for 1 hour. Subsequently, lung sections were washed with Stop/Wash Buffer for 10 minutes and treated with anti-digoxigenin conjugate for 30 minutes at room temperature. Colors were developed in liquid DAB+ Substrate Chromogen System (K3468, Dako North America). The nuclei were counterstained using Fast Red Substrate Kit (75×) (ab64254, Abcam). Images were taken using Nikon eclipse Ti-S inverted

phase contrast fluorescent microscope (Nikon Corp., Tokyo, Japan), and TUNEL index was calculated.

The Lung Genomics Research Consortium (LGRC) Cohort. Gene expression data for the *NTN1* gene were measured at the probe-level (probe ID: 8004880), from the Affymetrix Human Gene 1.0 ST Array (Affymetrix, Santa Clara, CA), used in the LGRC cohort as previously described (12). . Data from individuals with IPF and controls were used for this analysis. The gene expression data is available on the GEO database (http://www.ncbi.nlm.nih.gov/geo/) under the accession number GSE32539. Demographic characteristics of the LGRC cohort are listed in Table 1.

Statistics. Statistical analyses are fully outlined in the main text.

Supplementary Table S1. IPF subjects studied in survival analysis.

N	89
Age (years)	71.93 ± 6.58
Male sex	89 (100))
Race and Ethnicity, n (%)	
Caucasian	83 (93.26)
African American	3 (3.37)
Hispanic	3 (3.37)
Smoking Status n (%)	
Ever/Current	73 (82.02)
Never	16 (17.98)
FVC% at enrollment (percent predicted mean ± SD)	74.53 ± 17.78
$D_{LCO\%}$ at enrollment (percent predicted mean ± SD)	44.18 ± 16.25

GAP Index at enrollment (percent predicted mean ± SD)	4.47 ± 1.29

Data are presented as mean ± standard deviation (SD). FVC% = percent predicted forced vital capacity. $D_{LCO\%}$ = percent predicted diffusion capacity of the lung for carbon monoxide. GAP = gender, age, physiology.

Supplementary Table S2. Antibodies used for vibratome-based immunofluorescence

Name	Host/Iso-type	Cat. No.	Vendor ID	Dilution	Function
Primary antibody					
Rabbit TH polyclonal antibody	Rabbit/IgG	ab112	Abcam	1:100	Labeling TH-expressing adrenergic neurons
Mouse PGP9.5 monoclonal antibody	Mouse/IgG2a	ab8189	Abcam	1:100	Serving as a pan-neuronal marker for colocalization staining
Mouse α-SMA monoclonal antibody	Mouse/ IgG2a	ab7817	Abcam	1:250	Labeling airways and vessels
Secondary antibody					
Alexa Fluor™ 488 goat anti-rabbit IgG (H+L)	Goat / IgG	A11008	Invitrogen	1:500	For the labeling and visualization of rabbit primary antibody
Alexa Fluor™ 555 goat anti-mouse IgG (H+L) staining	Goat / IgG	A21422	Invitrogen	1:500	For the labeling and visualization of mouse primary antibody

Supplementary Table S3. Antibodies used for Imaging Mass Cytometry.

Target	Metal	Cat. No.	Clone No.	Vendor ID	Species reactivity	Dilution
CD11b	149Sm	3149028D	EPR1344	Fluidigm	Mouse Human	1:150
Netrin-1	152Sm	ab201324	EPR5428	Abcam	Human, Mouse, Rat	1:50
F4/80	159Tb	123102	BM8	Biolegend	Mouse	1:50
HistoneH3	176Yb	3176023D	D1H2	Fluidigm	Human, Mouse	1:300

Supplementary Table S4. Antibodies used for FACS.

Name	Host/Iso-type	Cat. No.	Vendor ID	Dilution	Function
Surface antibody					
CD45 mAb (30-F11), FITC	Rat / IgG2b, kappa	11-0451-82	eBioscience	1:100	For compensation
PE Rat Anti-Mouse CD45	Rat / IgG2b, kappa	553081	BD Biosciences	1:100	For compensation
CD45 mAb (30-F11) PerCP	Rat / IgG2b, kappa	45-0451-82	eBioscience	1:1000	For compensation and gating CD45+/-cells
CD45 mAb (30-F11), APC	Rat / IgG2b, kappa	17-0451-82	eBioscience	1:100	For compensation
Anti-ADRA1A antibody [EPR9691(B)] (Alexa Fluor® 647)	Rabbit / IgG	ab225190	Abcam	1:5000	For ADRA1A receptor expression
Anti-ADRA1B antibody [EPR10336]	Rabbit / IgG	ab169523	Abcam	1:1000	For ADRA1B receptor expression
Anti-ADRA1D antibody	Rabbit / IgG	PA5-77286	Invitrogen	1:100	For ADRA1D receptor expression
PE Rat Anti-Mouse CD31	Rat/ IgG2a	553373	BD Biosciences	1:100	Labeling endothelial cells
CD326 (EpCAM) mAb (G8.8), APC	Rat / IgG2a, kappa	17-5791-82	Invitrogen	1:200	Labeling epithelial cells
PE Rat Anti-CD11b	Rat (DA) IgG2b, κ	557397	BD Biosciences	1:800	Labeling macrophages
CD11c mAb (N418), PerCP-Cyanine5.5	Armenian hamster / IgG	45-0114-80	eBiosciences	1:800	Labeling lung macrophages

F4/80 mAb (BM8), APC	Rat / IgG2a, kappa	17-4801-82	Invitrogen	1.5:100	Labeling macrophages
Intracellular antibody					
FITC anti-mouse CD206 (MRC1) Antibody	Rat / IgG2a, kappa	141704	Biolegend	1.5:100	Labeling M2-like macrophage in mouse lungs
Goat Anti-Type I Collagen	Goat/ IgG	1310-01	SouthernBiotech	1:100	For collagen I expression
Netrin 1-FITC	Mouse/IgG2a	NB600-1344F	Novus biologicals	1:200	For NTN1 expression
Secondary antibody					
Alexa Fluor® 647 Donkey anti-rabbit IgG- (minimal x-reactivity) Antibody	Donkey/Polyclonal IgG	406414	Biolegend	1:2000	For the labeling of rabbit antibodies including antibodies against ADRA1A, ADRA1B and ADRA1D.
Isotype antibody					
FITC Rat IgG2a, κ	Rat/IgG2a, κ	RTK2758	Biolegend	1.5:100	Isotype control for FITC anti-mouse CD206 (MMR) Antibody
Goat IgG	Goat/IgG	0109-01	SouthernBiotech	1:100	Isotype control for goat anti-type I Collagen
Mouse IgG2a-FITC	Mouse/IgG2a	0103-02	SouthernBiotech	1:200	Isotype control for Netrin-1 FITC

Supplemental References

1. Hadi T, Boytard L, Silvestro M, Alebrahim D, Jacob S, Feinstein J, Barone K, Spiro W, Hutchison S, Simon R, et al. Macrophage-derived netrin-1 promotes abdominal aortic aneurysm formation by activating MMP3 in vascular smooth muscle cells. *Nat Commun.* 2018;9(1):5022.
2. Sun H, Zhu Y, Pan H, Chen X, Balestrini JL, Lam TT, Kanyo JE, Eichmann A, Gulati M, Fares WH, et al. Netrin-1 Regulates Fibrocyte Accumulation in the Decellularized Fibrotic Sclerodermatous Lung Microenvironment and in Bleomycin-Induced Pulmonary Fibrosis. *Arthritis Rheumatol.* 2016;68(5):1251-61.

3. Xie T, Liang J, Liu N, Huan C, Zhang Y, Liu W, Kumar M, Xiao R, D'Armiento J, Metzger D, et al. Transcription factor TBX4 regulates myofibroblast accumulation and lung fibrosis. *J Clin Invest.* 2016;126(8):3063-79.
4. Clausen BE, Burkhardt C, Reith W, Renkawitz R, and Forster I. Conditional gene targeting in macrophages and granulocytes using LysMcre mice. *Transgenic Res.* 1999;8(4):265-77.
5. Peng X, Moore M, Mathur A, Zhou Y, Sun H, Gan Y, Herazo-Maya JD, Kaminski N, Hu X, Pan H, et al. Plexin C1 deficiency permits synaptotagmin 7-mediated macrophage migration and enhances mammalian lung fibrosis. *FASEB J.* 2016;30(12):4056-70.
6. Zhou Y, Peng H, Sun H, Peng X, Tang C, Gan Y, Chen X, Mathur A, Hu B, Slade MD, et al. Chitinase 3-like 1 suppresses injury and promotes fibroproliferative responses in Mammalian lung fibrosis. *Sci Transl Med.* 2014;6(240):240ra76.
7. Nguyen KD, Qiu Y, Cui X, Goh YP, Mwangi J, David T, Mukundan L, Brombacher F, Locksley RM, and Chawla A. Alternatively activated macrophages produce catecholamines to sustain adaptive thermogenesis. *Nature.* 2011;480(7375):104-8.
8. Giesen C, Wang HA, Schapiro D, Zivanovic N, Jacobs A, Hattendorf B, Schuffler PJ, Grolimund D, Buhmann JM, Brandt S, et al. Highly multiplexed imaging of tumor tissues with subcellular resolution by mass cytometry. *Nat Methods.* 2014;11(4):417-22.
9. Schapiro D, Jackson HW, Raghuraman S, Fischer JR, Zanotelli VRT, Schulz D, Giesen C, Catena R, Varga Z, and Bodenmiller B. histoCAT: analysis of cell phenotypes and interactions in multiplex image cytometry data. *Nat Methods.* 2017;14(9):873-6.
10. Grebe KM, Takeda K, Hickman HD, Bailey AL, Embry AC, Bennink JR, and Yewdell JW. Cutting edge: Sympathetic nervous system increases proinflammatory cytokines and exacerbates influenza A virus pathogenesis. *J Immunol.* 2010;184(2):540-4.
11. Muramatsu I, Taniguchi T, and Okada K. Tamsulosin: alpha1-adrenoceptor subtype-selectivity and comparison with terazosin. *Jpn J Pharmacol.* 1998;78(3):331-5.
12. Yang IV, Coldren CD, Leach SM, Seibold MA, Murphy E, Lin J, Rosen R, Neidermyer AJ, McKean DF, Groshong SD, et al. Expression of cilium-associated genes defines novel molecular subtypes of idiopathic pulmonary fibrosis. *Thorax.* 2013;68(12):1114-21.

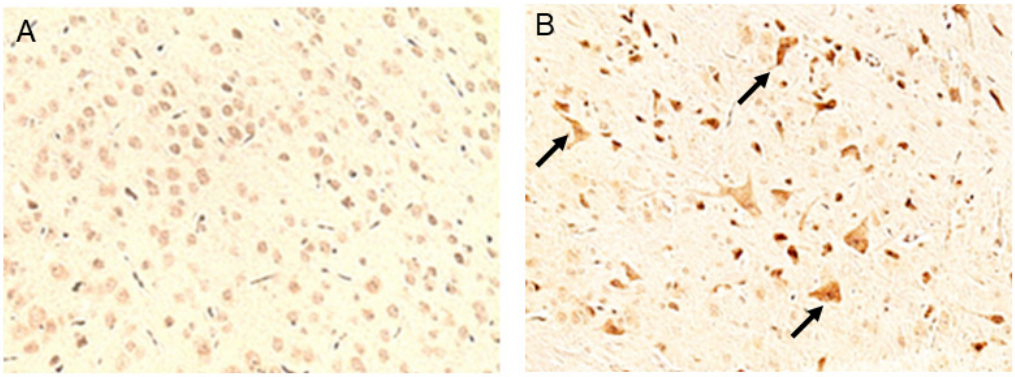

Supplementary Figure S1. Antibody controls for Netrin-1 immunohistochemistry. (A) NTN1 antibody shows minimal staining in archived lung tissues from the brain of a hypomorphic *Ntn1* mouse (*Ntn1*$^{+/-}$). This panel shows negative control for antibody specificity. (B) NTN1 antibody shows specific cellular staining in the *Ntn1*$^{+/+}$ mouse brain. This panel shows the positive control for antibody staining. Black arrows denote NTN1.

.

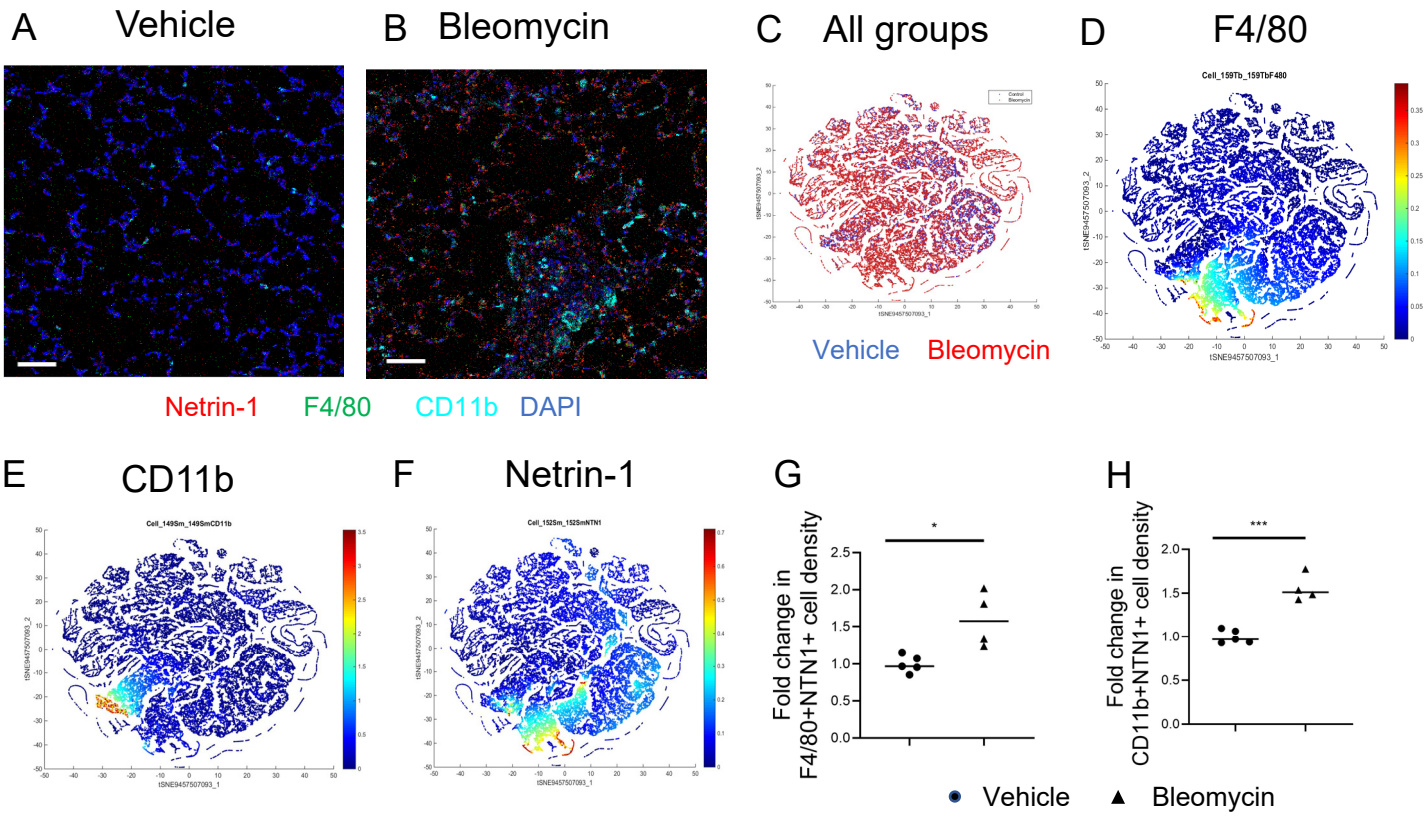

Supplementary Figure S2. Detection of Netrin-1, F4/80, and CD11b by Imaging Mass Cytometry. (**A and B**) Representative multiparametric images generated using pseudocoloring of channels. For the purposes of this analysis, four channels are shown (red: netrin-1, green: F4/80, cyan: CD11b, blue: DNA/histone H3) in vehicle (**A**) and bleomycin (**B**) challenged lungs. Scale bar is 50 microns. (**C**) Overlay of T-distributed Stochastic Neighbor Embedding (t-SNE) plots generate separate clusters based on marker heterogeneity in vehicle (blue) and bleomycin exposed (red) merged groups. (**D-F**) Heat maps of F4/80 (**D**), CD11b (**E**), and netrin-1 (**F**) expression applied to tSNE clustering of merged groups. Netrin-1 colocalizes with both markers., though additional populations of NTN1+ cells are also observed (**G** and **H**) Dot plot of fold change in the total number of F4/80+NTN1+ (**G**) and CD11b+NTN1+ (**H**) cells per mm^2 in the dataset. Round symbol: vehicle. Triangle: bleomycin. For G and H, **P*<0.05, ****P*<0.001 for bleomycin vs. vehicle.

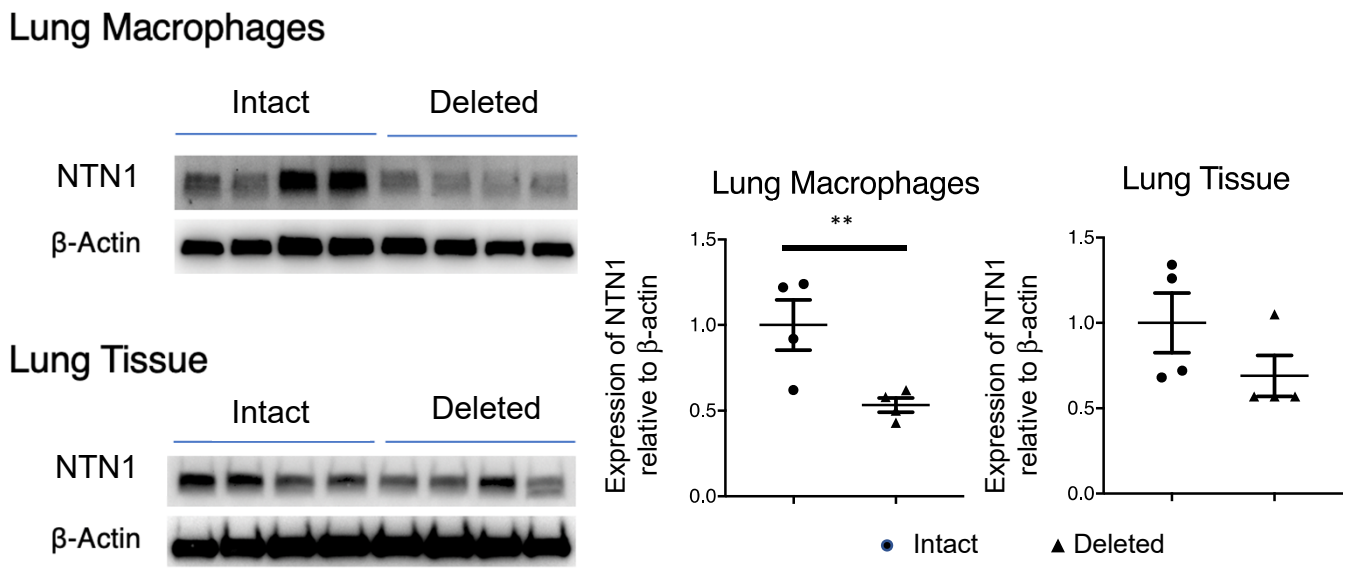

Supplementary Figure S3. Evaluation of NTN1 by Western blotting of isolated lung macrophages or whole lung tissue from mice with an intact or deleted *Ntn1* locus reveals robust and specific deletion in macrophages. The relative abundance of NTN1 vs. β-actin was calculated by densitometric analyses. Data are shown as fold change, mean ± SEM. $^{**}P < 0.01$.

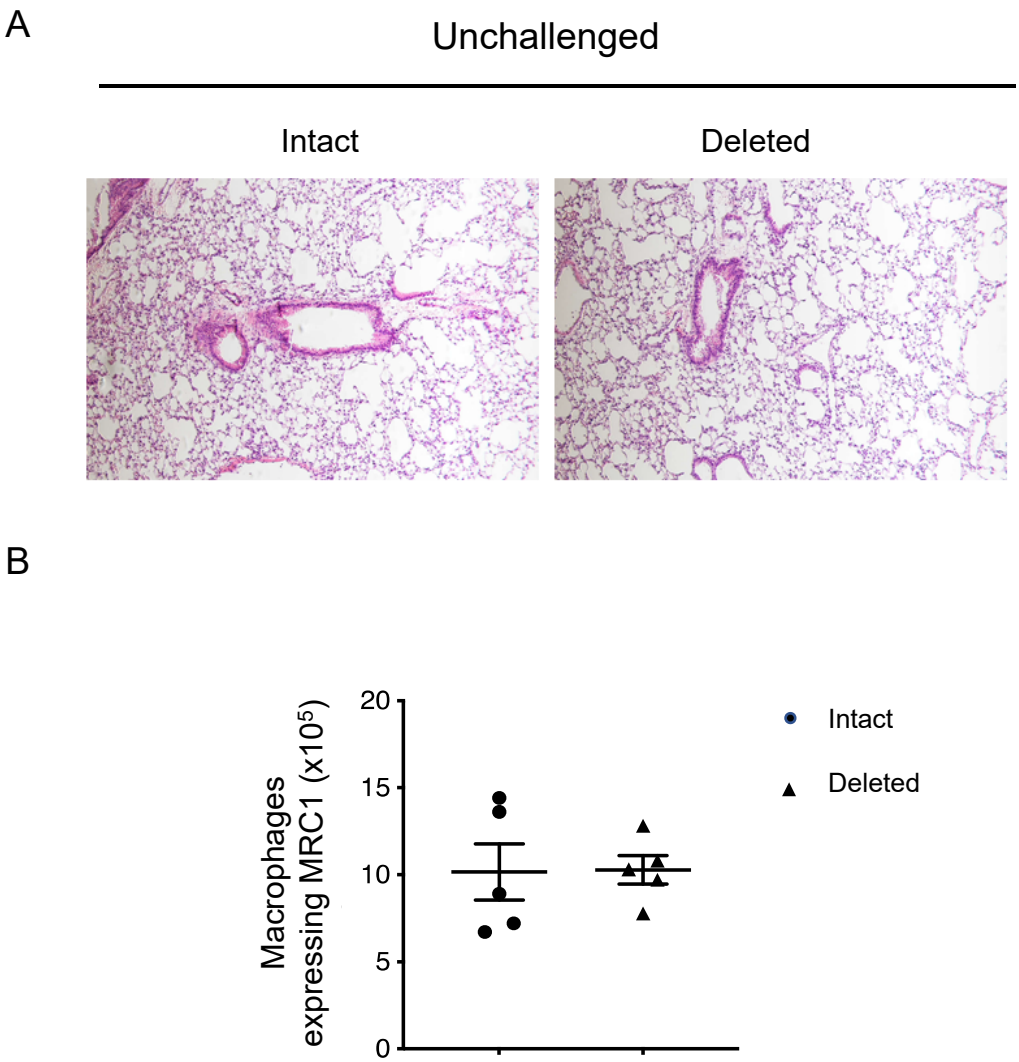

Supplementary Figure S4. (A) Comparison of H&E stained unchallenged lungs from mice with *Ntn1* intact or deleted in *LysM*+ cells reveals no obvious difference. The magnification is 10×. **(B)** Comparison of F4/80+CD11b+CD11c+ macrophages expressing MRC1 enumerated by FACS of lung suspensions reveals no obvious difference. Data are shown as mean ± SEM.

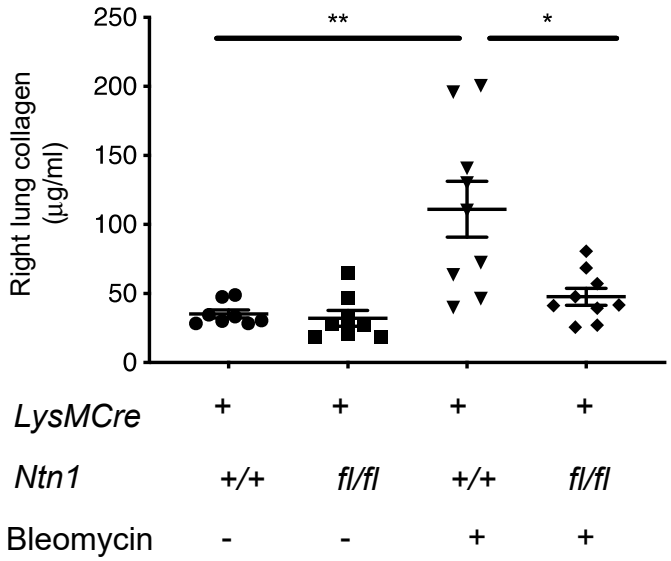

Supplementary Figure S5. Comparison of right lung collagen content in vehicle or bleomycin challenged mice in which *Ntn1* is intact or deleted in *LysM*+ cells. Round symbol: vehicle challenged *LysMCre, Ntn1*$^{+/+}$. Square: vehicle challenged *LysMCre, Ntn1*$^{fl/fl}$. Triangle: bleomycin challenged *LysMCre, Ntn1*$^{+/+}$. Diamond: bleomycin challenged *LysMCre, Ntn1*$^{fl/fl}$. For ease of interpretation, significance is only noted for comparisons of interest. **P*<0.05, ***P*<0.01. Data are shown as mean ± SEM.

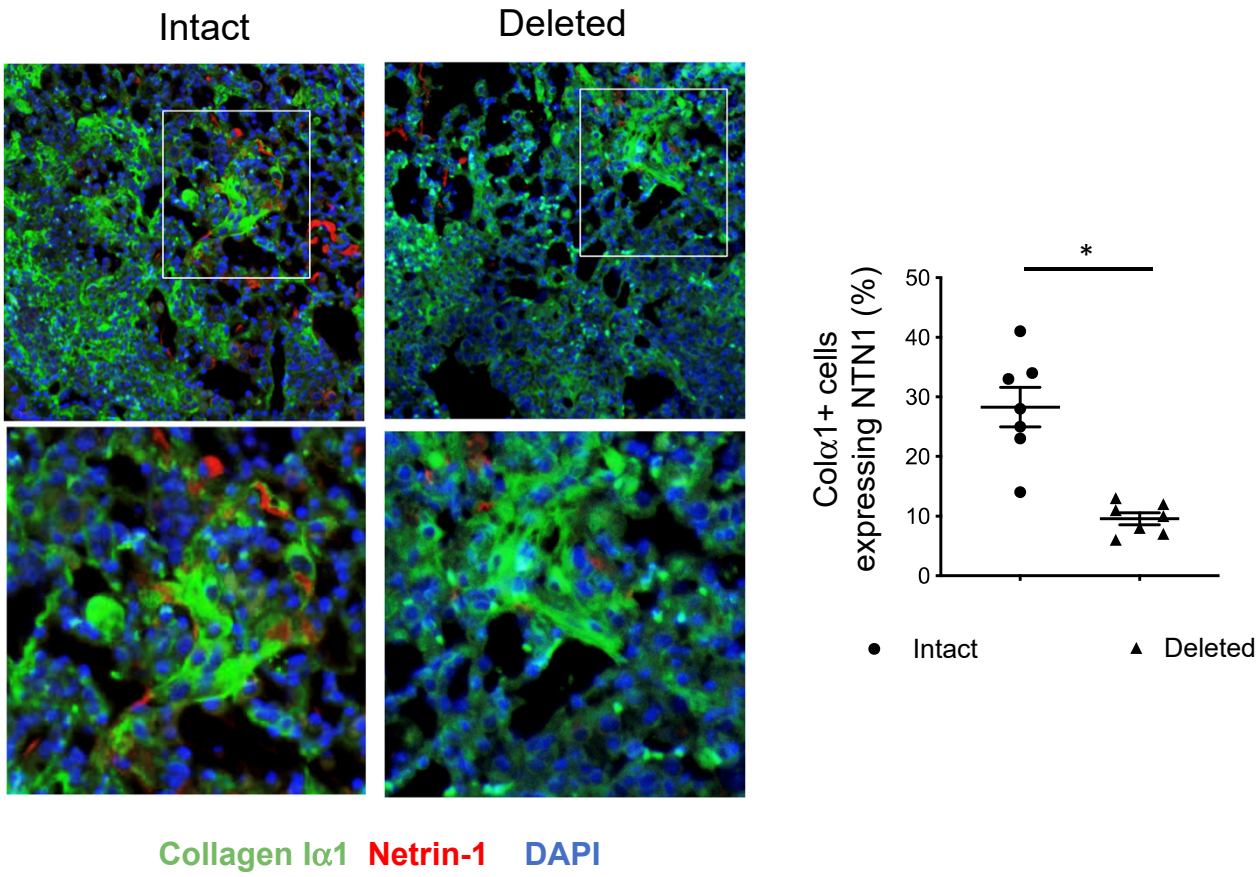

Supplementary Figure S6. Immunofluorescence evaluation of lungs obtained from *ColIα2-CreER, Ntn1*$^{fl/fl}$ mice treated with corn oil ("intact," round symbol) or Tamoxifen ("deleted," triangle) reveals reduced NTN1 detection in fibroblasts (identified here by Col1α1). Top: low power view. Bottom: enlarged boxed region. Green: Collagen1α1, red: NTN1, blue: DAPI. 10× original magnification. Data are shown as mean ± SEM. **P*<0.05.

.

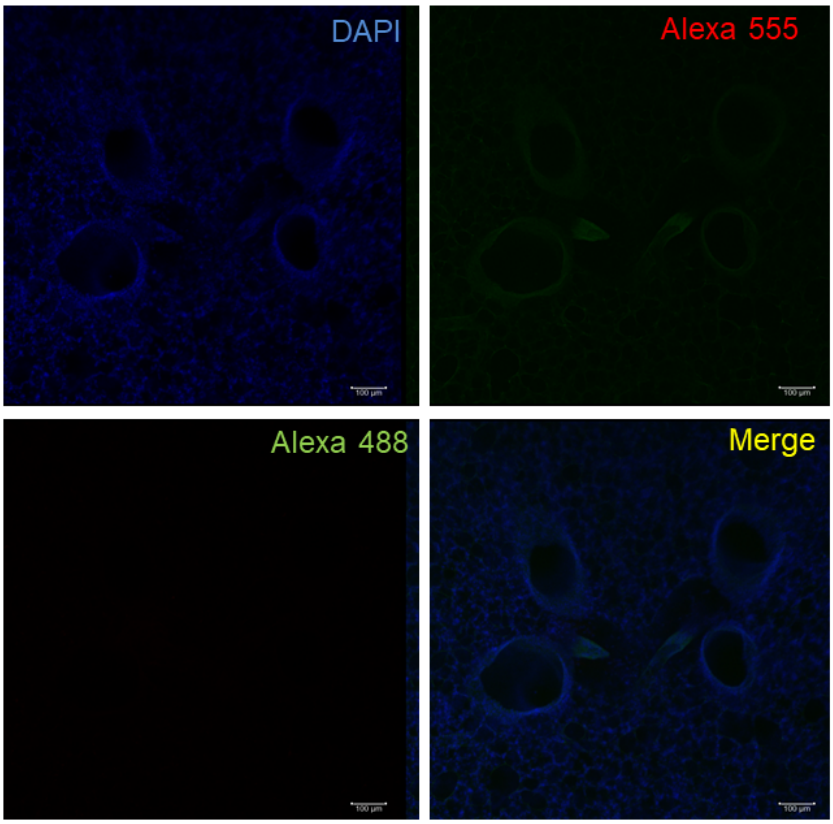

Supplementary Figure S7. Negative control for immunostaining. Sections stained with only goat anti-mouse IgG (Alexa Fluor® 555 conjugate) and goat anti-rabbit IgG (Alexa Flour® 488 conjugate) secondary antibodies show absent signal in the red, green, and merged (yellow) channels. Slides are counterstained with DAPI (blue). Scale bar = 100 microns.

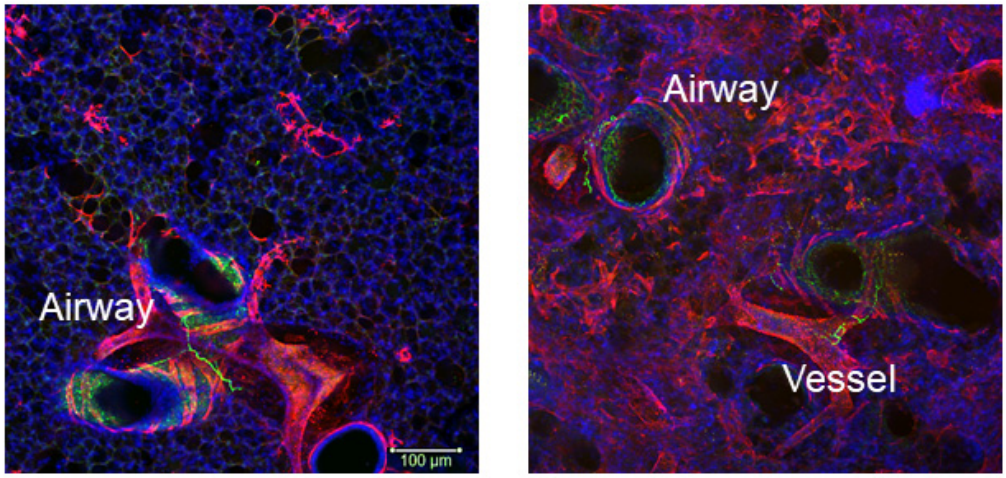

Supplementary Figure S8. Additional images of vehicle (left) and bleomycin (right) challenged WT mouse lungs stained for αSMA (red), TH (green) and DAPI (blue). These images were chosen to demonstrate TH+ staining in the airways and blood vessels of bleomycin exposed animals. They do not show parenchymal TH+ nerve-like structures. Scale bar = 100 microns.

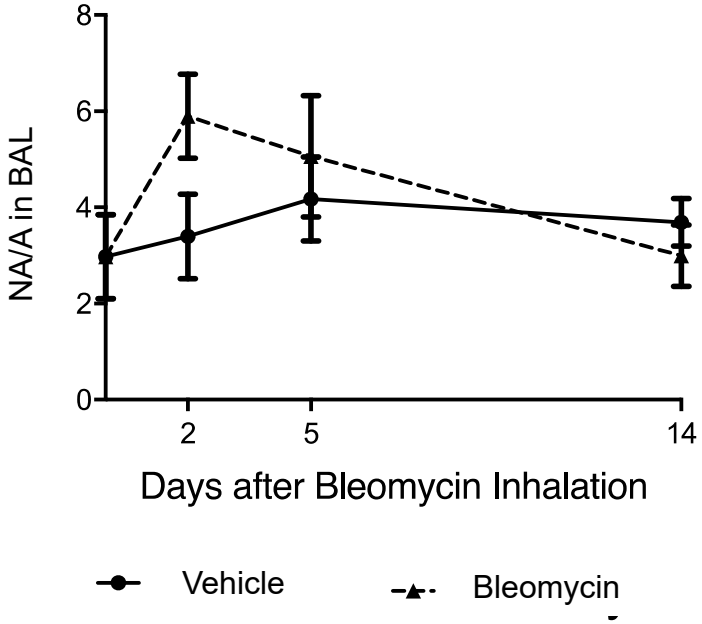

Supplementary Figure S9. Kinetics of the noradrenaline (NA) to adrenaline (A) ratio in vehicle (solid line) and bleomycin (dotted line) challenged mouse bronchoalveolar lavage (BAL) fluid. BAL NA/A is not significantly altered at any timepoint. Data are shown as mean ± SEM.

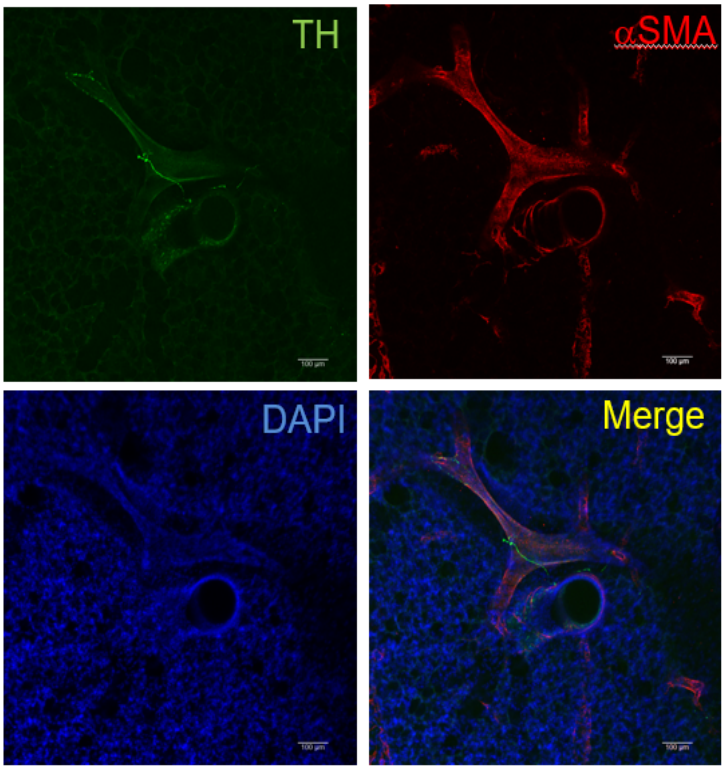

Supplementary Figure 10. Baseline TH staining in *LysMCre, Ntn1*$^{fl/fl}$ mouse lungs. Shown are TH (green label), αSMA (red label), DAPI (blue label) and merged image (yellow label). Scale bar = 100 microns.

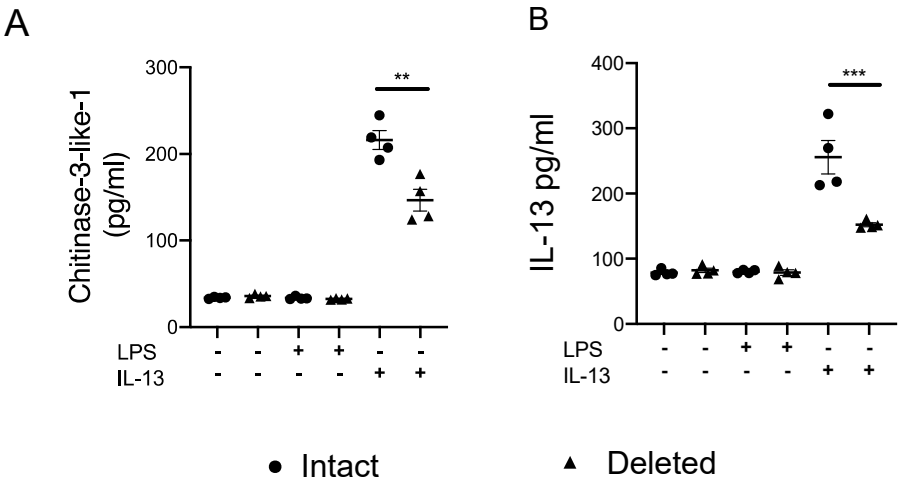

Supplementary Figure S11. Cytokine concentrations in supernatants from *Ntn1* deficient peritoneal macrophages. Peritoneal macrophages with *Ntn1* deleted show reduced concentrations of Chi3L1 following stimulation with IL-13 (A). IL-13 levels in supernatants are also reduced (B). Data are shown as mean ± SEM, ***P*<0.01, ****P*<0.001.

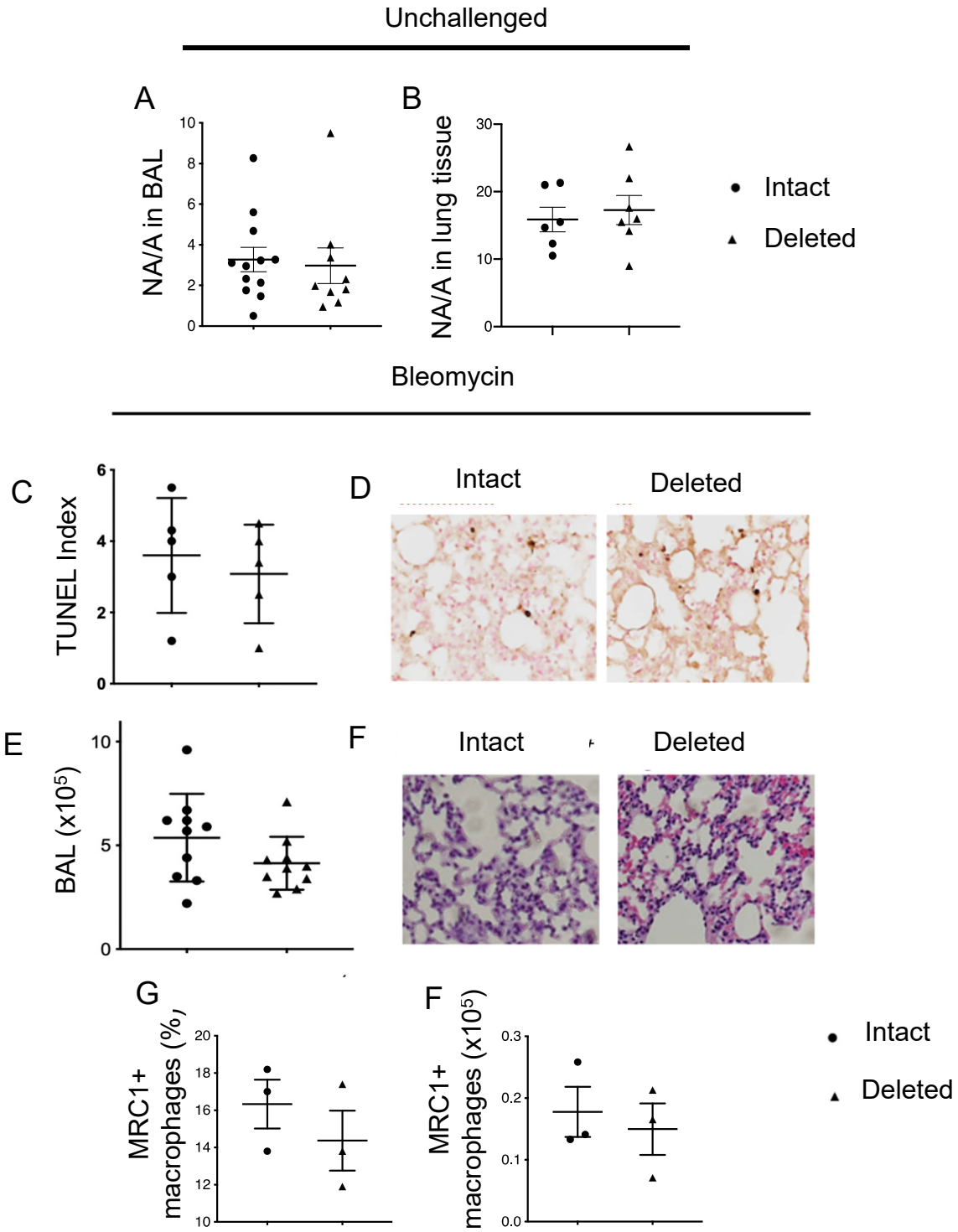

Supplementary Figure S12. Effect of *Ntn1* deficiency on bleomycin induced injury, inflammation, and MRC1+ macrophage accumulation. **(A** and **B)** Deletion of *Ntn1* deletion has no effect on the ratio of Noradrenaline to Adrenaline (NA/A) in the BAL **(A)** or lung tissue **(B)** of unchallenged mice. **(C-E)** there is also no effect on cell death measured by TUNEL staining 48 hours after bleomycin. **(E)** comparison of groups. **(D, E)** 10× image of TUNEL staining denoted by brown nuclear signal counterstained with nuclear fast red in the lungs of mice with myeloid *Ntn1* intact (**D**) or deleted (**E**). **(F-H)** *Ntn1* deletion in *LysM*+ cells has no effect on lung inflammation or injury measured by BAL cell counts **(H)** and H&E staining *(***G, H***)* 5 days after bleomycin. Original image 10×. **(I, J)** *Ntn1* deletion in *LysM*+ cells has no obvious effect on quantities **(I)** or proportions of MRC1+ macrophages **(J)** 14 days following bleomycin. In all panels, data are shown as mean ± SEM.

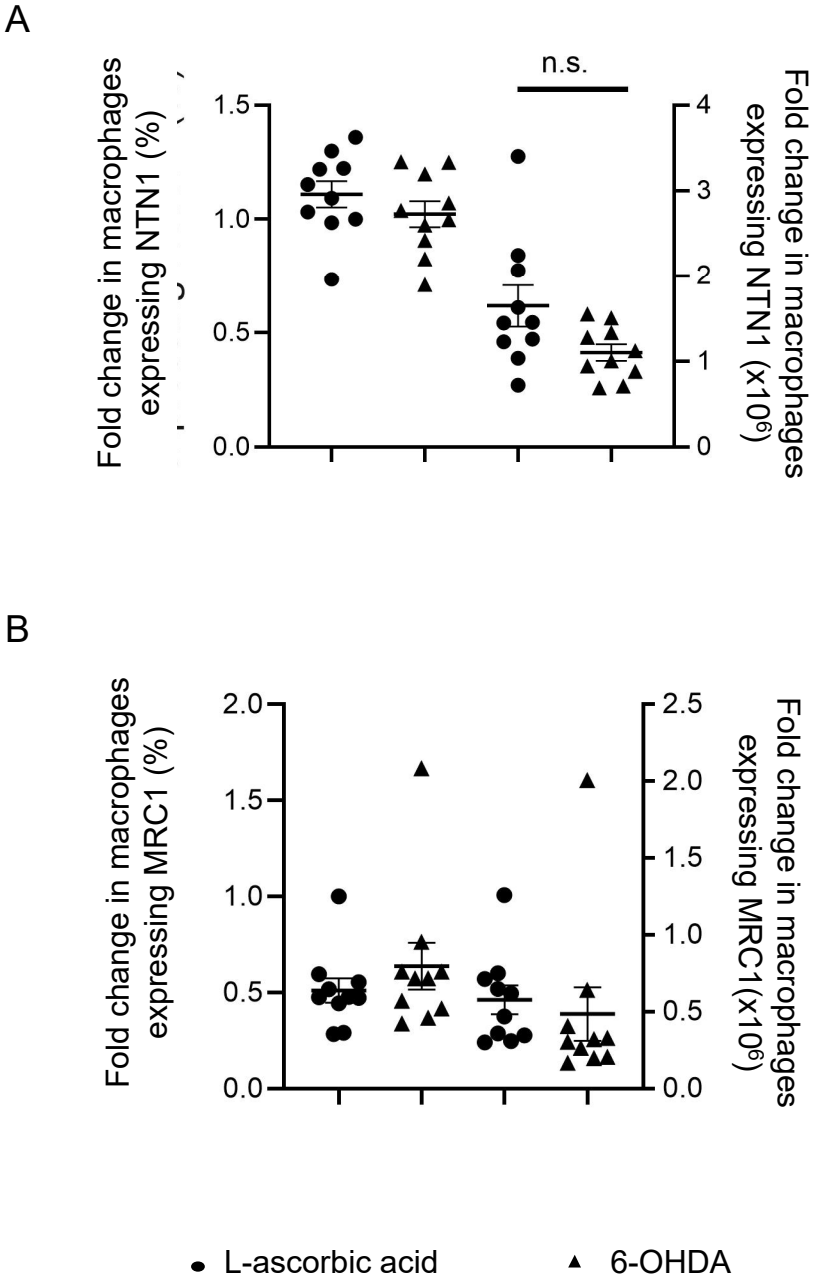

Supplementary Figure S13. Effect of chemical sympathectomy on macrophage phenotypes. Relative to WT mice treated with the vehicle control L-ascorbic acid (round symbol), WT mice subject to chemical denervation with the sympathetic neurotoxin 6-OHDA show unchanged percentages (left axis) and quantities (right axis) of macrophages expressing either NTN1 (A) or MRC1 (B).

A

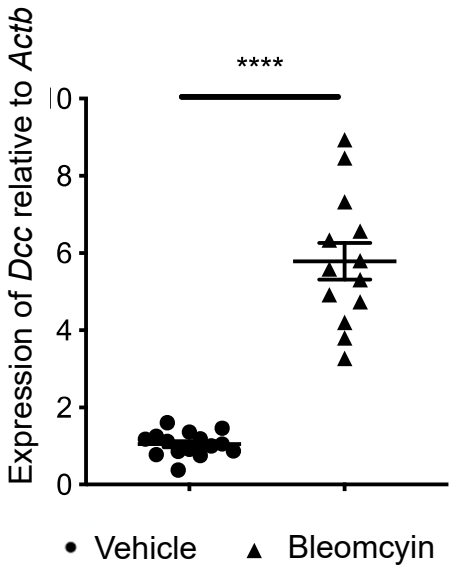

B

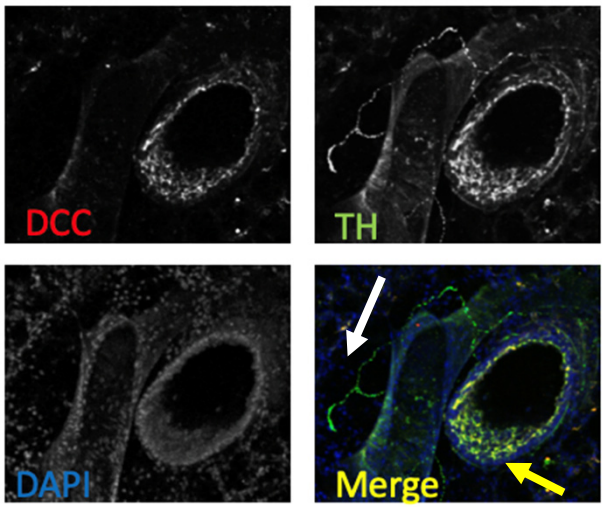

Supplementary Figure S14. DCC expression in the mouse lung. **(**A**)** The expression of *Dcc* relative to *Actb* is increased in whole lung lysates 14 days after bleomycin. ****P<0.0001. (B) Confocal imaging of DCC (red), TH (green) and DAPI (blue) shows that DCC colocalizes with TH in the lumen (yellow arrow) but not exterior (white arrow) of airways.

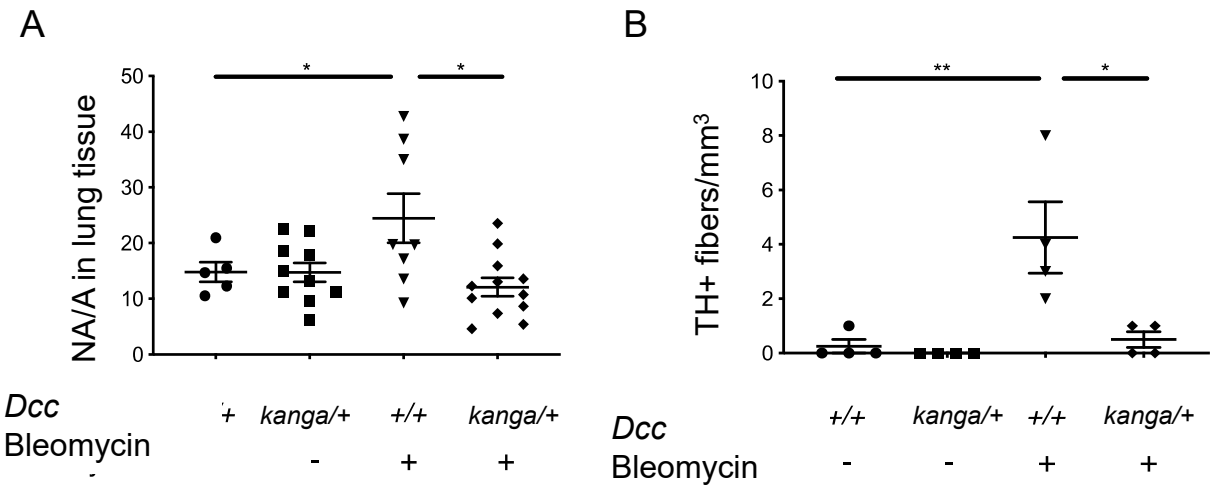

Supplementary Figure S15. Effect of *Dcc* deficiency on fibrotic endpoints. (A and B) Relative to $Dcc^{+/+}$ mouse lungs, $DCC^{kanga/+}$ mouse lungs contain reduced lung tissue NA/A **(A)** and parenchymal detection of TH+ nerves **(B)** 14-days following bleomycin. Round symbol: vehicle challenged $Dcc^{+/+}$. Square: vehicle challenged $Dcc^{kanga/+}$. Triangle: bleomycin challenged $Dcc^{+/+}$. Diamond: vehicle challenged $Dcc^{kanga/+}$. $*P<0.05$, $**P<0.01$.

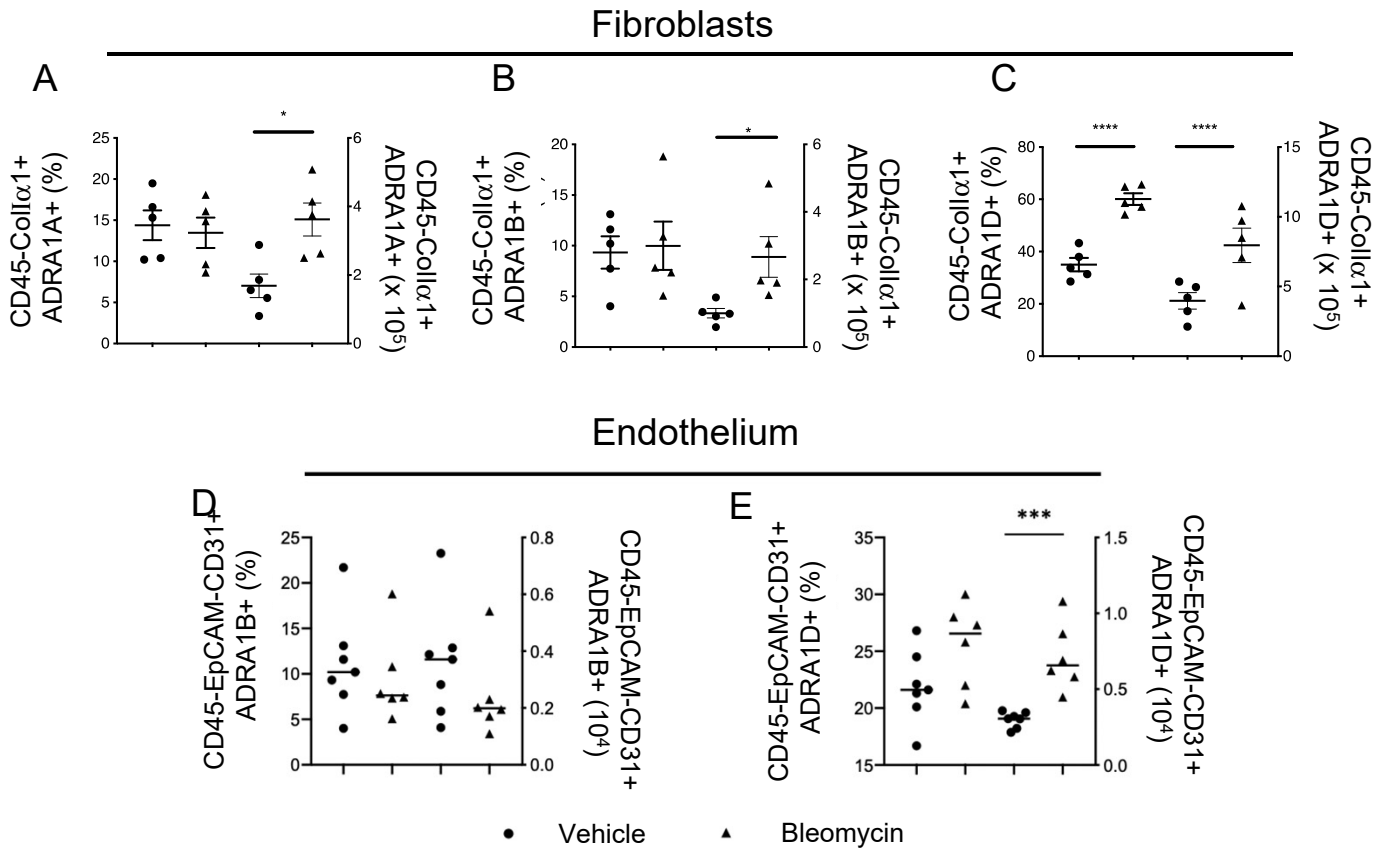

Supplementary Figure S16. Evaluation of α1 adrenergic receptor subtypes on fibroblasts and endothelial cells in WT lungs. (**A-C**) Expression of ADRA1A, ADRA1B, and ADRA1D on CD45-CollIα1+ fibroblasts detected by FACS of lung suspensions. Percentages of cells expressing ADRA1A (**A**) and ADRA1B (**B**) are unchanged, while ADRA1D percentages (**C**) are increased. In contrast, a significant increase in the total number of fibroblasts expressing ADRA1A (**A)**, ADRA1B (**B)** and ADRA1D (**C)** is seen following bleomycin (all comparisons with two-tailed Student's t-test). (**D** and **E**) Expression of ADRA1B and ADRA1D on CD45-EpCAM-CD31+ endothelial cells detected by FACS of lung suspensions. Percentages and quantity of cells expressing ADRA1B (**D**) are unchanged. Percentages of ADRA1D+ endothelial cells (**E**) are unchanged (left), but overall cell quantities (**E**) increase (right). *P<0.05, **P<0.01, ***P<0.001, ****P<0.0001.

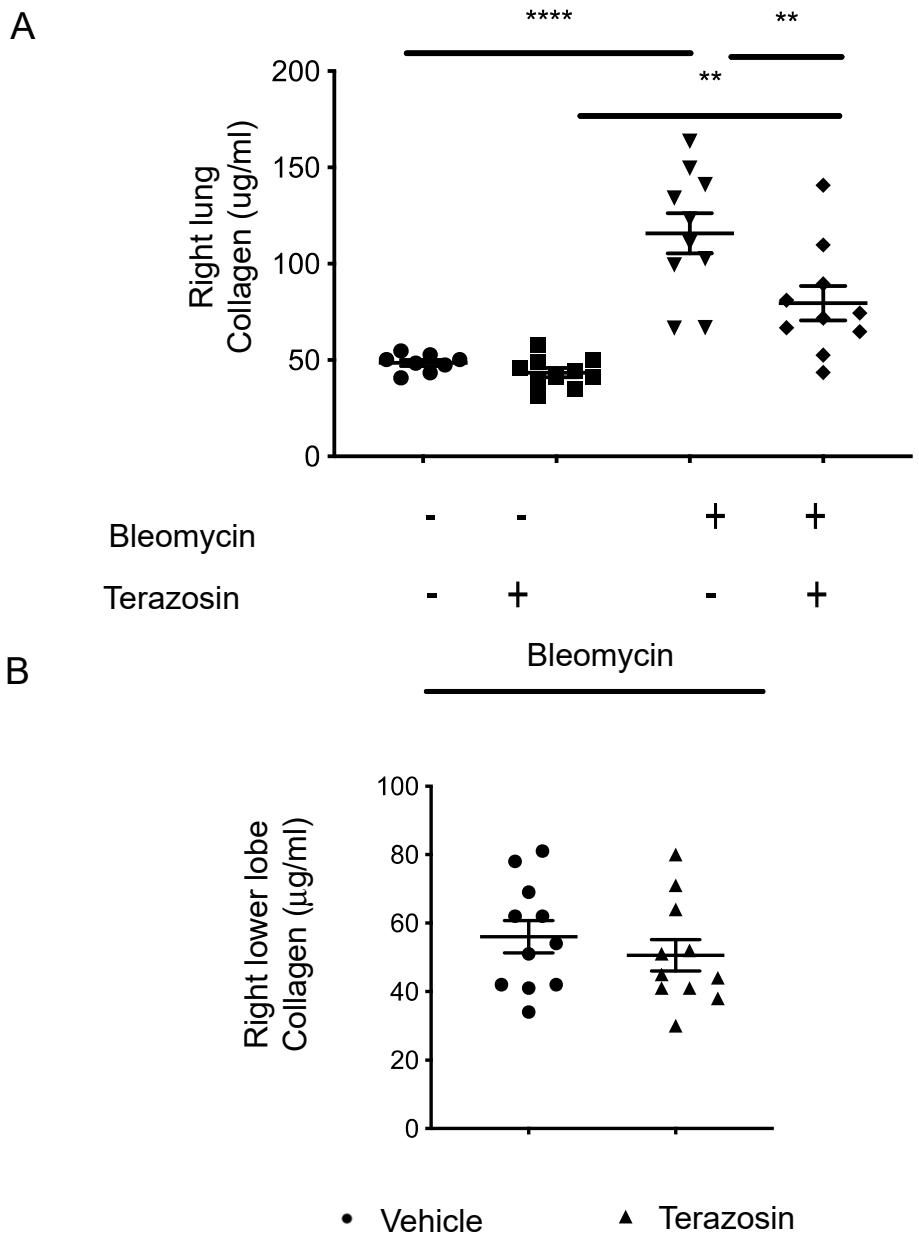

Supplementary Figure S17. Treatment with Terazosin can suppress but not reverse bleomycin induced lung fibrosis. **(A)** Relative to vehicle treated mice, treatment with the α_1 adrenoreceptor antagonist Terazosin started 5 days after bleomycin reduces right lung collagen content at the 14-day timepoint after bleomycin. (**B**) In contrast, Terazosin treatment started at day 10 following bleomycin does not impact right lower lobe collagen at the 21 day timepoint. Data are shown as mean ± SEM. ***P*<0.01, *****P*<0.0001.

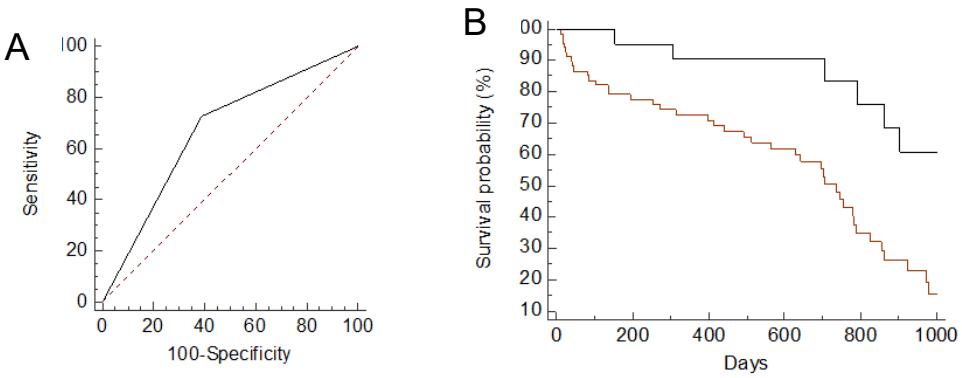

Supplementary Figure S18. Alpha$_1$ adrenoreceptor antagonism in IPF. (A) Receiver operator curve (ROC) analysis reveals α1 adrenoreceptor antagonist use can reliably dichotomize subjects for all-cause mortality. **(B)** Unadjusted Kaplan Meier analysis comparing patients taking the α1 adrenoreceptor antagonists (Terazosin or Tamsulosin, black line, n=22) with those not on such therapy (red line, n=67).